

Dark matter annihilation rates with velocity-dependent annihilation cross sections

Brant E. Robertson^{1,2} and Andrew R. Zentner³

¹ *Kavli Institute for Cosmological Physics, and Department of Astronomy and Astrophysics, University of Chicago, 933 East 56th Street, Chicago, IL 60637, USA*

² *Enrico Fermi Institute, 5640 South Ellis Avenue, Chicago, IL 60637, USA*

³ *Department of Physics and Astronomy, University of Pittsburgh, Pittsburgh, PA 15260, USA*

(Dated: October 14, 2019)

The detection of byproducts from particle annihilations in galactic halos would provide important information about the nature of the dark matter. Observational evidence for a local excess of high-energy positrons has motivated recent models with an additional interaction between dark matter particles that can result in a Sommerfeld enhancement to the cross section. In such models, the cross section for annihilation becomes velocity-dependent and may enhance the dark matter annihilation rate in the solar neighborhood relative to the rate in the early universe sufficiently to source observed fluxes of high-energy positrons. We demonstrate that, for particle interaction cross-sections that increase with decreasing velocity, the kinematical structures of dark matter halos with interior density profiles shallower than isothermal, such as Navarro-Frenk-White or Einasto halos, may induce a further enhancement owing to the position-dependent velocity distribution. We provide specific examples for the increase in the annihilation rate with a cross-section enhanced by the Sommerfeld effect. In dark matter halos like that of the Milky Way and Local Group dwarf galaxies, the effective cross section at the halo center can be significantly larger than its local value. The additional enhancement owing to halo kinematics depends upon the parameters of any model, but is a prediction of certain models aimed at explaining measured positron fluxes and can exceed an order of magnitude.

PACS numbers: 98.35.+d, 98.62.Gq, 98.35.Gi, 14.80.Ly

I. INTRODUCTION

Astrophysical probes are important elements of the effort to identify the cosmological dark matter (DM). Detecting γ -rays from DM annihilation is a prime scientific motivation for existing and forthcoming γ -ray instruments including the space-based Fermi Gamma-ray Space Telescope (FGST) [1], and atmospheric detectors such as the High Energy Stereoscopic System (HESS) [2], the Very Energetic Radiation Imaging Telescope Array System (VERITAS) [3], the Major Atmospheric Gamma-ray Imaging Cerenkov telescope (MAGIC & MAGIC II) [4], the Collaboration of Australia and Nippon for Gamma-ray Observatory in the Outback (CANGAROO) [5], the High-Altitude Water Cerenkov experiment (HAWC) [6], and the Whipple 10m [1, 7, 8, 9]. The unexpected positron excess above 10 GeV detected by the Payload for Anti-matter Exploration and Light-Nuclei Astrophysics (PAMELA) satellite [10] and the cosmic ray electron/positron excess at $\sim 300 - 800$ GeV detected by the Advanced Thin Ionized Calorimeter (ATIC) instrument [11] have been interpreted as products of DM annihilation in the halo of the Milky Way and driven significant interest in leptophilic particle DM models with suppressed hadronic production channels (e.g., Refs. [12, 13]).

The DM annihilation interpretation of the PAMELA and ATIC data faces a challenge in that the required cross section is roughly an order of magnitude or more larger than the value $\langle\sigma v\rangle \sim 3 \times 10^{26} \text{ cm}^3 \text{ s}^{-1}$ necessary for a thermal relic to have the observed contempo-

rary DM density [12, 14, 15, 16]. A class of proposals that gives rise to large effective cross sections in galactic halos introduces an attractive force among dark matter particles mediated by a relatively light boson. The annihilation cross section can be large courtesy of a non-perturbative correction called the ‘‘Sommerfeld enhancement’’ [13, 17, 18, 19, 20, 21, 22]. The new force effectively focuses incident plane-wave wavefunctions and can result in a significant increase in the effective annihilation cross section. The sizes of these ‘‘Sommerfeld-enhanced’’ cross sections are very sensitive to the parameters of the model and are generally monotonically decreasing functions of relative encounter speed [13, 22].

While the antiparticle excesses may have a more pedestrian astrophysical origin [26, 27], Sommerfeld-enhanced DM annihilation yields interesting phenomenology. Annihilation rates scale as $\Gamma \propto \langle\sigma v\rangle\rho^2$ where $\langle\sigma v\rangle = \int f(v)\sigma(v)v dv$ is the cross section times velocity averaged over the distribution of particle velocities $f(v)$, and ρ is the local density. In canonical DM particle scenarios, $\sigma(v)v$ is constant at $v/c \ll 1$ and the integral is trivial. Previous estimates of the annihilation rates in Sommerfeld-enhanced models adopted a single characteristic velocity v_{char} to describe entire halos, approximating $\int f(v)\sigma(v)v dv \approx \sigma(v_{\text{char}})v_{\text{char}}$. This approach may sensibly address the local PAMELA/ATIC data but neglects other observational consequences of such models. Moreover, while the constant halo velocity approximation is valid in the case of isothermal halos where density depends upon radius as $\rho \propto r^{-2}$, the structures of dark matter halos are generally not isothermal (and not Maxwellian) and the velocity distribution will de-

pend upon position.

The spatially-dependent velocity scale in DM halos is intuitive. Cosmological simulations suggest that DM halos have density profiles that scale as $\rho(r) \sim r^{-1}$ in their interiors (e.g., Ref. [28, 29]). The characteristic speeds of particles then scale as $v_{\text{char}} \sim \sqrt{GM(<r)/r} \propto \sqrt{r}$, where $M(<r)$ is the mass contained within a sphere of radius r . Characteristic relative velocities decrease with radial position. As a consequence, the velocity dependence of the cross section can result in a position dependence in the annihilation rate beyond the standard $\Gamma \propto \rho^2(r)$ proportionality. We use the Sommerfeld enhancement to provide a popular example of a velocity-dependent cross section, but we emphasize that the simple point of this paper pertains to any model in which the annihilation cross-section is velocity dependent. Models in which s-wave annihilation is forbidden are another class of scenarios where annihilation cross sections can be velocity dependent, and such scenarios have been studied within the context of dark matter (a recent example in a similar context is Ref. [30]).

To calculate annihilation rates in cases of velocity-dependent interaction cross sections, an average over the radially-dependent velocity distribution should be performed. We perform this calculation and provide examples of the modified DM annihilation rates below. In particular we show that for some choices of parameters, the radial dependence of the velocity distribution can lead to important modifications to the radial dependence of the annihilation rate.

II. HALO DENSITY AND VELOCITY STRUCTURE

Navarro et al. [29] (NFW) found that the density profiles of DM halos in cosmological simulations scaled as $\rho(r) \propto r^{-1}$ at small radii and transitioned to $\rho(r) \propto r^{-3}$ in the halo exterior. We take the NFW density profile,

$$\rho(x) = \frac{4\rho_s}{x(1+x)^2}, \quad (1)$$

where $x \equiv r/r_s$ as one of our example halo models. The NFW profile has a scale density $\rho(x=1) = \rho_s$.

More recent numerical studies have demonstrated that the innermost density profiles of DM halos follow a radially-dependent power-law slope that may soften relative to the NFW $\gamma = 1$ value. Navarro et al. [33] find that the function

$$\rho(x) = \rho_s \exp\left[-\frac{2}{\eta}(x^\eta - 1)\right] \quad (2)$$

with $\eta \sim 0.17$ represents well the DM halos formed in their simulations. This function has a form similar to the distribution suggested by Einasto [34], and we refer to Equation 2 as the Einasto profile. This density profile has a local power-law index $d \ln \rho / d \ln r|_{x=1} = 2$ and density $\rho(x=1) = \rho_s$.

The left panel of Figure 1 shows the density profile for two example galactic DM halos. Constraints on the rotation curve of the Milky Way (MW) suggest that its DM halo has a virial mass of $M_{\text{vir}} \approx 10^{12} M_\odot$, halo concentration $C_{\text{vir}} \equiv R_{\text{vir}}/r_s \sim 12$, and scale length $r_s \sim 22$ kpc [31]. These parameters imply a DM density at the MW scale radius of $\rho_s \sim 10^6 M_\odot \text{ kpc}^{-3}$. In addition to the MW, we consider annihilation in the halo of the Local Group satellite galaxy Ursa Minor because it subtends a large angle on the sky and should be among the most luminous dwarf galaxies in DM annihilation products [32]. Stellar kinematics constrain the Ursa Minor halo to have $r_s \approx 0.6$ kpc and $\rho_s \approx 1.1 \times 10^8 M_\odot \text{ kpc}^{-3}$ [32].

For a spherically-symmetric system with an isotropic distribution of velocities, the equilibrium one-dimensional velocity dispersion σ_v can be computed from the Jeans equation [35],

$$\sigma_v^2(r) = \frac{1}{\rho} \int_\infty^r \rho \frac{d\Phi}{dr} dr, \quad (3)$$

where Φ is the total gravitational potential supplied by all components of the galaxy, including structures other than that for which the dispersion is being computed. The right panel of Figure 1 shows the velocity dispersion $\sigma_v(x)$ for models of the MW and Ursa Minor DM halos modeled with NFW and Einasto density profiles. The NFW halo models reach a density $\sim 100\times$ larger than the Einasto profile models at $x \sim 10^{-6}$, and have significantly lower inner velocity dispersions. Halos with structures similar to the Ursa Minor satellite have halo velocity dispersions ~ 5 times smaller than the MW. In what follows, we adopt these values as fiducial parameters for the halos of the MW and Ursa Minor.

For the interaction of two particles with velocities \mathbf{v}_1 and \mathbf{v}_2 , the collision rate is proportional to the integral

$$\langle \sigma v \rangle = \int \sigma(v_{\text{rel}}) v_{\text{rel}} f(\mathbf{v}_{\text{rel}}) d^3 \mathbf{v}_{\text{rel}}, \quad (4)$$

where $\mathbf{v}_{\text{rel}} \equiv \mathbf{v}_1 - \mathbf{v}_2$. The relative velocity distribution $f(v_{\text{rel}})$, which depends on the local halo velocity dispersion $\sigma_v(x)$, can be computed from the individual velocity distributions of particles by changing variables from \mathbf{v}_1 and \mathbf{v}_2 to \mathbf{v}_{rel} and the center-of-mass velocity $\mathbf{v}_{\text{cm}} = \mathbf{v}_1 + \mathbf{v}_2$ and integrating over \mathbf{v}_{cm} and the directional dependence of \mathbf{v}_{rel} .

To illustrate the importance of the radial dependence of σ_v , we approximate the velocity distribution function as an isotropic Maxwellian distribution with dispersion $\sigma_v \ll v_{\text{esc}} \equiv \sqrt{-2\Phi}$. In this case, the relative velocity distribution is simply

$$f(v_{\text{rel}}) = v_{\text{rel}}^2 \frac{1}{2\sqrt{\pi}\sigma_v^3} \exp\left(-\frac{v_{\text{rel}}^2}{4\sigma_v^2}\right). \quad (5)$$

We emphasize here that we utilize this form as a matter of convenience. Halo velocity distributions generally exhibit both velocity anisotropy and deviations from the Maxwellian form, but can be calculated directly from the

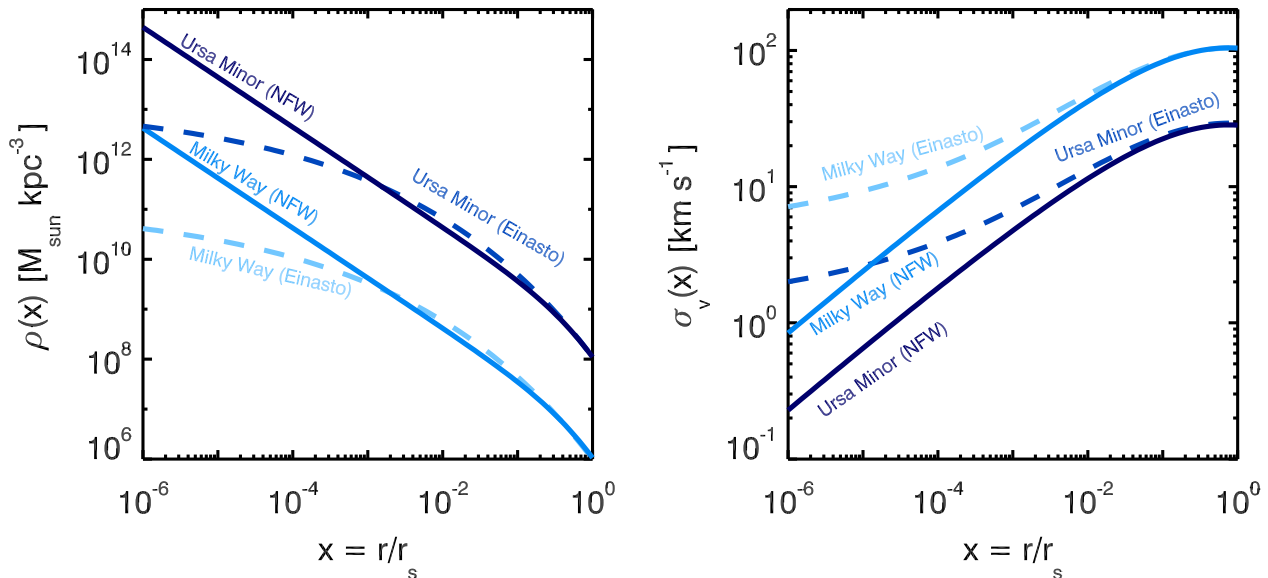


FIG. 1: Halo density (left panel) and velocity dispersion (right panel) profiles as a function of radius in units of halo scale radii, $x = r/r_s$. We show NFW (*solid lines*) and Einasto (*dashed lines*) models of a Milky Way-like halo with parameters $M_{\text{vir}} \approx 10^{12} h^{-1} M_{\odot}$, and $r_s \approx \text{kpc}$ [31] as well as the Local Group dwarf galaxy Ursa Minor with $\rho_s \approx 1.1 \times 10^8 M_{\odot} \text{ kpc}^{-3}$, and $r_s = 0.6 \text{ kpc}$ [32].

distribution function (see § 4 or Ref. [35]). For our purposes, the Maxwellian approximation should be conservative since the kurtosis of the velocity distribution in the halo models we adopt increases beyond the Gaussian value at radii $x \lesssim 0.1$ [see, e.g., 36] and would result in a further enhancement of the annihilation rate for the cross section velocity-dependence we consider below. We expect that the effect of velocity anisotropy will be to introduce geometrical factors of order unity into the evaluation of Eqn. 4 by altering the form of the distribution function.

III. SOMMERFELD CROSS SECTION ENHANCEMENT

As we argue above, if the particle interaction cross section has some additional velocity dependence beyond the standard $\langle \sigma v \rangle \sim \text{constant}$, the kinematical structure of the DM halo may alter the annihilation rate. In what follows, we consider the Sommerfeld enhancement of annihilation cross sections as a particular example of a velocity-dependent annihilation cross section of significant current interest.

The Sommerfeld [17] enhancement describes the increase in the effective cross section owing to an attractive force between incident particles. Let $\psi(r)$ denote the radial wavefunction of the equivalent one-body problem relative to the center-of-mass. The annihilation rate should be proportional to $|\psi(r)|^2$ in a region near the origin. The Sommerfeld enhancement is an increase in the

annihilation rate when the wavefunction $\psi(r)$ near the origin is significantly altered owing to an additional, relatively long-range interaction. Let $\psi_0(r)$ and σ_0 be the radial wavefunction and annihilation cross section absent any new long-range force. Upon introduction of the new force, the effective cross section is shifted to $\sigma = S\sigma_0$, where $S = |\psi(r=0)|^2/|\psi_0(r=0)|^2$ is the Sommerfeld factor. The Sommerfeld factor can be calculated from the attenuation of the solution $\psi(r)$ using the optical theorem as [13, 20, 22]

$$S = \frac{|\psi(\infty)|^2}{|\psi(0)|^2}. \quad (6)$$

If we assume s-wave ($\ell = 0$) annihilation in the non-relativistic limit, then the scattering wavefunction is a solution to the Schrödinger equation in the form,

$$\frac{1}{m_{\text{DM}}} \frac{d^2 \psi(r)}{dr^2} - V(r) \psi(r) = -m_{\text{DM}} \left(\frac{v}{c}\right)^2 \psi(r), \quad (7)$$

where m_{DM} is the DM particle mass. If the attractive force has a finite range, Eq. (7) can be solved numerically using the boundary condition that far from the origin the particle is a free wave, and

$$\psi(r \rightarrow \infty) \propto \exp\left(i \frac{m_{\text{DM}} v}{c} r\right). \quad (8)$$

Once the solution to $\psi(r)$ is integrated inward to $r \rightarrow 0$, the velocity-dependent Sommerfeld enhancement can be evaluated from Eq. (6).

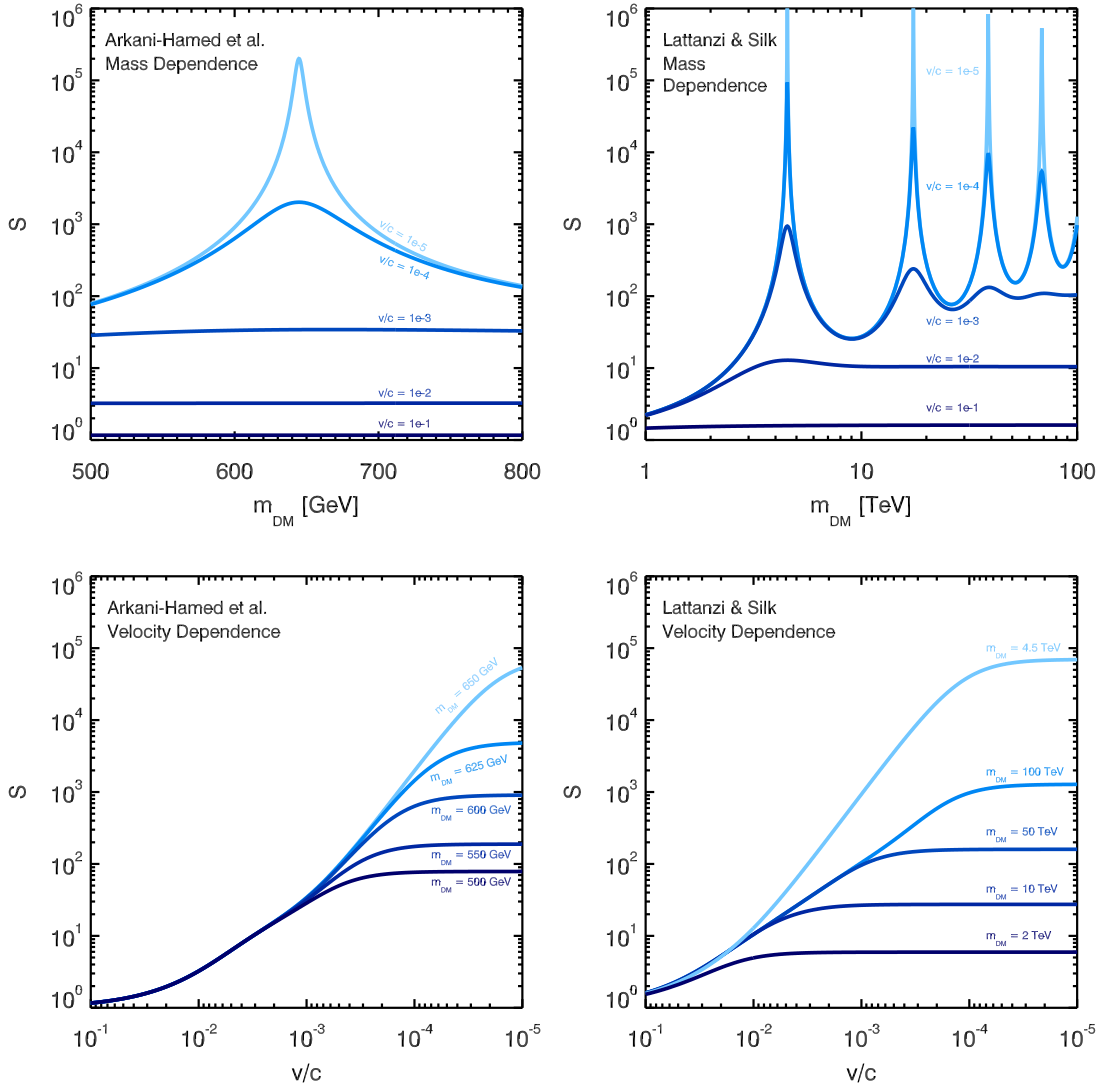


FIG. 2: Sommerfeld enhancement to the interaction cross section for annihilation using the parameters of the Arkani-Hamed et al. [13] model (*left column*, $\alpha \approx 0.01$, $m_V \sim 1$ GeV) and Lattanzi and Silk [22] model (*right column*, $\alpha \approx 1/30$, $m_V \approx 90$ GeV). We show the cross section enhancement as a function of DM particle mass m_{DM} (*upper row*) or particle velocity (*lower row*). The right panels reproduce the results shown in Figures 2 and 3 of Lattanzi and Silk [22].

For definiteness, we take the interaction to be given by an attractive Yukawa potential

$$V(r) = -\frac{\alpha}{r} \exp(-m_V r) \quad (9)$$

where $\alpha > 0$ is the coupling strength and m_V is the mass of the boson that mediates the new force. This useful model for understanding the phenomenology of the Sommerfeld effect has been explored in Refs. [13, 22]. S can be large when $v/c \ll \alpha$ and saturates to a maximum value for relative speeds

$$v/c \ll \sqrt{\alpha m_V / m_{\text{DM}}}. \quad (10)$$

Large enhancements require $\sqrt{\alpha m_V / m_{\text{DM}}} \lesssim v/c \lesssim \alpha$.

In general, bound states exist when $m_{\text{DM}}/m_V \sim n^2/\alpha$, where n is an integer, and lead to large, resonant effective cross section enhancements.

For our demonstration, we assume that the cross section can be written as $\sigma(v)v = (\sigma v)_0 S(v)$ where $(\sigma v)_0$ is independent of velocity and the Sommerfeld factor $S(v)$ contains the entire velocity dependence. In the Yukawa model, the Sommerfeld factor additionally depends on the ratio, m_V/m_{DM} . As relevant examples, we will use the DM model parameters of Arkani-Hamed et al. [13] ($\alpha = 10^{-2}$, $m_V = 1$ GeV, and $m_{\text{DM}} = 500 - 800$ GeV) and Lattanzi and Silk [22] ($\alpha = 1/30$, $m_V = 90$ GeV, and $m_{\text{DM}} = 1 - 100$ TeV). The parameters of Ref. [13] were chosen to match the mass scale of several hundred

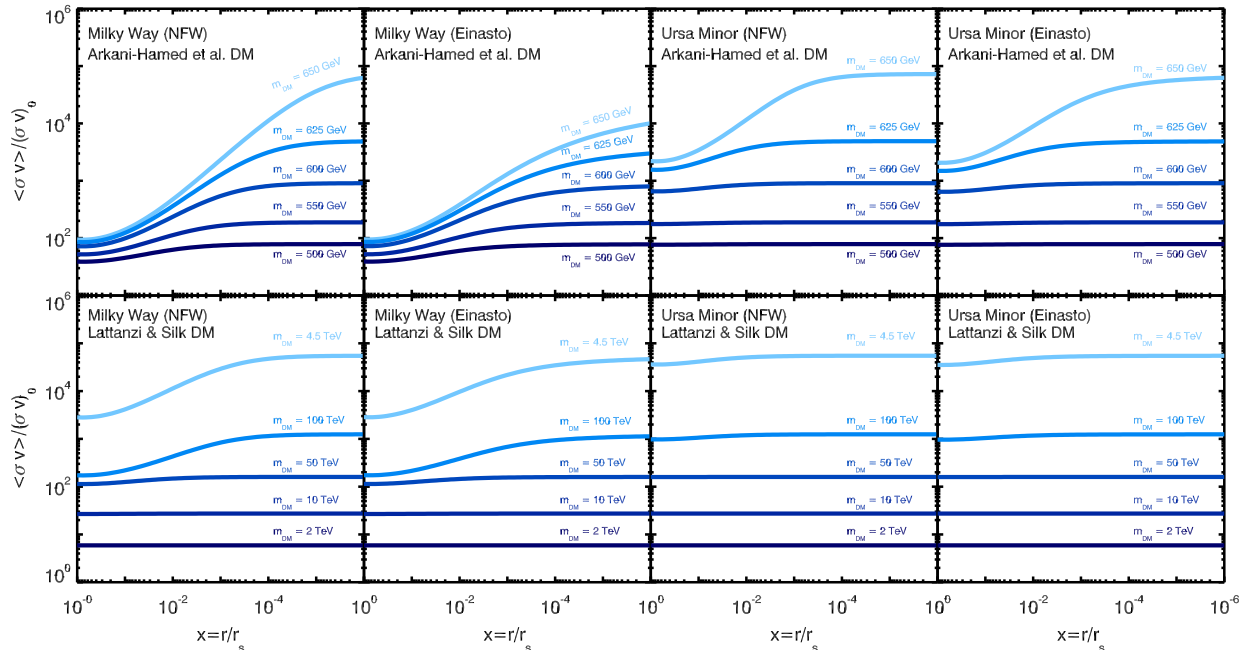


FIG. 3: Radial enhancement in the DM annihilation rate owing to a Sommerfeld-like velocity-dependent cross section and the radially-dependent halo velocity dispersion σ_v . Shown are the products of cross section and velocity averaged over the local velocity distribution function and normalized to their values absent any Sommerfeld effect, $\langle\sigma v\rangle/\langle\sigma v\rangle_0 = \int S(v)f(v)dv$. Position is given in units of halo scale radii, $x = r/r_s$. The annihilation enhancement is plotted for MW-like (*left panels*) and Ursa Minor-like (*right panels*) halos with NFW (*1st and 3rd columns*) and Einasto (*2nd and 4th columns*) halo profiles, using either the Arkani-Hamed et al. [13] or Lattanzi and Silk [22] DM parameters.

GeV selected by the ATIC data [11] while also satisfying Eq. (10) so that large boosts are attainable ($v/c \lesssim 10^{-3}$ in the local dark matter halo). The Ref. [22] parameters are based on the same considerations for large S -factors obtained via an interaction mediated by Z boson exchange. Though we make specific choices including the form of the interaction and the masses of particles, this method can be applied to any model of particle interactions. The qualitative features we describe hold for Sommerfeld-enhanced annihilation in general.

Figure 2 shows the dependence of the Sommerfeld enhancement on the dark matter particle masses and relative velocities (the right panels of Fig. 2 reproduce the results in Figures 2 and 3 of Ref. [22]). Sommerfeld factors can clearly be quite large for reasonable parameter values. The upper panels of Fig. 2 show examples of resonant capture at specific values of m_{DM} . The lower panels show that the Sommerfeld factor becomes unimportant as $v/c \rightarrow 1$ and saturates according to Eq. (10). For $\alpha \gtrsim v/c \gtrsim \sqrt{\alpha m_V/m_{\text{DM}}}$ the Sommerfeld factor exhibits a strong relative speed dependence. $S(v) \propto v^{-1}$ for models away from resonance while $S(v) \propto v^{-2}$ near resonances [13, 22].

IV. THE ENHANCEMENT OF VELOCITY-DEPENDENT DARK MATTER ANNIHILATION IN GALACTIC HALOS

Figure 3 shows the enhancement of the annihilation cross section owing to the Sommerfeld effect as a function of position in dark matter halos. We show the quantity $\langle\sigma(v)v\rangle/\langle\sigma v\rangle_0 = \int S(v)f(v)dv$, which amounts to the Sommerfeld factor averaged over the relative velocity distribution functions for dark matter halo models at each position within the halo. We show halo models representative of the MW and the Ursa Minor satellite for the dark matter parameters chosen by Arkani-Hamed et al. [13] and Lattanzi and Silk [22].

The behavior of the annihilation enhancement $\langle\sigma v\rangle/\langle\sigma v\rangle_0$ depends on the halo kinematical structure and the details of the particle model. If the DM particle mass is near resonance, the Sommerfeld enhancement increases faster than $S(v) \propto v^{-1}$ and the decline of the halo velocity dispersion with radius leads to a large increase in the annihilation rate between the radii $x \sim 1$ and $x \sim 0$ in addition to the expected $\Gamma \propto \rho^2$ dependence. The relative increase is larger for the Milky Way ($\langle\sigma v\rangle_{x \sim 0}/\langle\sigma v\rangle_{x \sim 1} \sim 10^3$ for Arkani-Hamed et al. [13] DM with mass $m_{\text{DM}} \approx 650$ GeV) than for Ursa Minor ($\langle\sigma v\rangle_{x \sim 0}/\langle\sigma v\rangle_{x \sim 1} \sim 30$) because the velocity dispersion of Ursa Minor near $x \sim 1$ is already approaching the

velocity at which the Sommerfeld boost saturates. The faintest known Local Group dwarfs such as SEGUE 1 [37] or Coma Berenices [38] with very low velocity dispersions ($\sigma_v \lesssim 10$ km/s, see Martinez et al. [39]) will have a radially-dependent cross section enhancement only if the saturation velocity is very low ($v/c \lesssim 10^{-5}$). When m_{DM} is such that the interactions are far from resonance, the effects are much less dramatic for the parameters we have chosen, but can be significantly larger in models with either smaller coupling strength α or larger m_{DM} , so that saturation occurs at significantly lower velocities as given by Eq. (10).

One aspect of Fig. 3 is worthy of explicit note in the context of recent proposals to explain the PAMELA/ATIC data with DM annihilations. In the MW halo, the diffusion length of multi-GeV positrons is short (\lesssim kpc) so that the relevant enhancement is the enhancement evaluated in a region local to the solar neighborhood, with $x \approx 0.35$. Fig. 3 indicates that for a fixed enhancement factor in the Solar neighborhood, the enhancement factor toward the Galactic center can vary significantly depending upon the specifics of the model. For these examples, the effective cross section at the Galactic center can be $\sim 10 - 10^3$ times larger than its local value.

Similarly, the case of Ursa Minor as an example of a Local Group dwarf satellite is interesting. Should observable γ -rays be produced in this satellite, the surface brightness profile will result from the position-dependent density *and* velocity distribution. In models with Sommerfeld enhancements, the radial gradient in the annihilation signal encodes information about the mass ratio m_V/m_{DM} . The scale radius of Ursa Minor subtends $\sim 2^\circ$ on the sky, and so this gradient may be a challenge to identify with an instrument such as FGST, with an angular resolution of ~ 10 arcminutes, but may be accessible to atmospheric Cerenkov detectors such as VERITAS, HESS, MAGIC, and CANGAROO with angular resolutions of the order of arcminutes.

V. DISCUSSION AND CONCLUSIONS

We have studied the influence of the kinematical structure of dark matter halos on dark matter annihilations in models with velocity-dependent annihilation cross sections. The methods we have used are general, but we have considered specific examples of the Sommerfeld enhancement to DM annihilations that have been proposed in order to explain recent measurements of high energy positron fluxes by PAMELA and ATIC. As our primary aim has been to illustrate the general importance of halo kinematics for velocity-dependent annihilations, we have cast our answers in terms of relative annihilation cross sections without specifying either a normalization of the cross section at high relative velocity $[(\sigma v)_0]$ or particular yields of outgoing leptons and photons from such annihilations. Our results demonstrate that the kinematical structure of DM halos can influence the annihilation rate

in important ways. In particular, the velocity distributions of dark matter particles may be a strong function of position so that velocity-dependent annihilation cross sections may give rise to annihilation rates that vary with halo position in addition to the dependence upon local number density $\Gamma \propto \rho^2(r)$. These results could easily be incorporated into cosmological N-body simulation estimates of dark matter annihilation rates [e.g., 40, 41].

Halo velocity structure may be important for annihilations within the MW. For the specific cases of Sommerfeld enhancements with the Arkani-Hamed et al. [13] and Lattanzi and Silk [22] DM parameter choices, halo kinematical structure leads to an effective DM annihilation cross section that rises by a factor of $\sim 10 - 10^3$ between the solar neighborhood and the MW halo center. The increase in the annihilation rate is most prevalent when the interaction occurs near resonance with $m_{\text{DM}} \sim n^2 m_V/\alpha$. In any case, the enhancement tends to a constant at small radii owing to the saturation of the Sommerfeld effect when condition Eq. (10) is met. This radial dependence can lead to relatively large boosts in annihilation products from the Galactic center relative to the local boost with or without taking additional boosts from halo substructure into consideration.

The examples that we have presented are simple, but we have studied more complete models of the Milky Way including the influence of the baryonic components of the Milky Way galaxy according to the parameterizations of Klypin et al. [31] and self-consistent models of Widrow and Dubinski [42]. In all cases, our qualitative result holds. The kinematical structure of the DM halo remains important in the sense that the Sommerfeld boost in the solar neighborhood can be significantly different from the boost elsewhere in the halo. What differs in these models are the detailed parametrics. For a specific set of dark matter interaction parameters, including the potential of the baryonic component of the Galaxy decreases the local Sommerfeld boost but increases the gradient of $\langle \sigma v \rangle / (\sigma v)_0$. Including a large black hole at the center of the Galactic potential leads to a cut-off in the enhancement level at roughly the radius of influence of the black hole, which is of order $r \sim 10^{-3} - 10^{-4} r_s$ and depends in detail upon the structural parameters one assumes for the galaxy and the halo. At this early stage, a detailed exploration of the parameter space seems of limited value, though we speculate that it may be more fruitful to seek such tests of velocity dependent cross sections in dwarf galaxies where there are fewer complications.

The dwarf satellites of the Milky Way may be additional sources of observable annihilation radiation that can shed light on the effective cross section for DM annihilation [13]. We have considered the case of the dwarf satellite Ursa Minor because it subtends a large solid angle on the sky and would be one of the most luminous of any known MW satellite in DM annihilation products [32]. Our results indicate that in systems like Ursa Minor the kinematical structure of the halo may reveal a signature of Sommerfeld-enhanced annihilation. In par-

ticular, models with large Sommerfeld enhancements to the dark matter annihilation cross section may result in a surface brightness profile that varies more rapidly than the density-squared weighting would imply over the inner few arcminutes of the galaxy. The scale over which the variation is significant is small compared to the angular resolution of FGST (~ 10 arcmin.), but comparable to that of atmospheric Cerenkov detectors such as HESS, MAGIC, VERITAS, and CANGAROO.

Of course, the absolute cross section for annihilation is not known, so models for which halo structure will be important are cases where the Sommerfeld factor is not yet in the saturation regime for a large fraction of the halo. In the case of the MW, a large radial gradient in the annihilation rate requires that saturation should occur at speeds less than the local DM velocity dispersion of $v/c \sim 10^{-3}$. For dwarf halos such as Ursa Minor the requirement is $v/c \lesssim 10^{-4}$, while smaller dwarfs like SEGUE 1 or Coma Berenices require saturation at $v/c \lesssim 10^{-5}$. For these conditions to be satisfied, either the coupling constant α or the mass ratio m_V/m_{DM} must be tuned to values many orders magnitude below unity. The Sommerfeld enhancement saturation explains why the spatial dependence of the effective cross section is mild in Ursa Minor for the Lattanzi and Silk [22] particle model shown in Fig. 3. Likewise, the first collapsing halos with masses for less than the halos of contemporary dwarf galaxies will lie well within the saturation regime (if $M \sim M_{\oplus}$, then $v/c \sim 10^{-8}$), so that constraints from γ -ray backgrounds owing to annihilation in these objects remain relevant [43, 44].

The position dependence of the annihilation cross section may be a testable prediction of Sommerfeld-enhanced DM annihilation models of the PAMELA/ATIC data in some regions of parameter

space. For the Milky Way, the decreasing width of the velocity distribution can result in far greater fluxes of annihilation products from the Galactic Center than would otherwise be expected. In the case of Ursa Minor, it might be possible to detect the signature of an effectively spatially-dependent annihilation cross section that varies on scales of \sim arcminutes. If the PAMELA/ATIC data have an astrophysical explanation [26, 27], the current motivation for Sommerfeld boosts would be diminished, but an enhancement owing to a velocity-dependent cross section for interactions among dark matter particles may still be possible. In such cases, the Sommerfeld boost may manifest solely as modified spatial profiles of γ -rays from halo particle annihilations. Either way, it is an exciting time in the quest to identify the dark matter and the flood of data expected over the next few years will only add to this excitement.

Acknowledgments

We are grateful to Babu Bhatt, Dan Hooper, Marc Kamionkowski, Savvas Koushiappas, Louis Strigari, and Amol Upadhye for useful discussions. This work was motivated in part by the Particle Cosmology Stimulus Package meeting between the University of Chicago and Fermilab. BER gratefully acknowledges support from a Spitzer Fellowship through a NASA grant administered by the Spitzer Science Center, and is partially supported by the Kavli Institute for Cosmological Physics at the University of Chicago. ARZ is supported by the University of Pittsburgh, by the National Science Foundation through grant AST 0806367, and by the Department of Energy.

-
- [1] S. Ritz, in *The First GLAST Symposium*, edited by S. Ritz, P. Michelson, and C. A. Meegan (2007), vol. 921 of *American Institute of Physics Conference Series*, pp. 3–7.
 - [2] W. Hofmann and H. E. S. S. Collaboration, in *International Cosmic Ray Conference (2003)*, vol. 5 of *International Cosmic Ray Conference*, pp. 2811–+.
 - [3] T. C. Weekes, in *Bulletin of the American Astronomical Society* (2005), vol. 37 of *Bulletin of the American Astronomical Society*, pp. 1402–+.
 - [4] D. Bastieri, in *37th COSPAR Scientific Assembly (2008)*, vol. 37 of *COSPAR, Plenary Meeting*, pp. 202–+.
 - [5] H. Kubo, A. Asahara, G. V. Bicknell, R. W. Clay, Y. Doi, P. G. Edwards, R. Enomoto, et al., *New Astronomy Review* **48**, 323 (2004).
 - [6] G. Sinnis and Hawc Collaboration, in *High Energy Gamma-Ray Astronomy*, edited by F. A. Aharonian, H. J. Völk, and D. Horns (2005), vol. 745 of *American Institute of Physics Conference Series*, pp. 234–245.
 - [7] F. Aharonian, A. G. Akhperjanian, A. R. Bazer-Bachi, M. Beilicke, W. Benbow, D. Berge, K. Bernlöhr, C. Boisson, O. Bolz, V. Borrel, et al., *Physical Review Letters* **97**, 221102 (2006), arXiv:astro-ph/0610509.
 - [8] F. Aharonian, A. G. Akhperjanian, A. R. Bazer-Bachi, M. Beilicke, W. Benbow, D. Berge, K. Bernlöhr, C. Boisson, O. Bolz, V. Borrel, et al., *Astroparticle Physics* **29**, 55 (2008), 0711.2369.
 - [9] M. Wood, G. Blaylock, S. M. Bradbury, J. H. Buckley, K. L. Byrum, Y. C. K. Chow, W. Cui, I. de la Calle Perez, A. D. Falcone, S. J. Fegan, et al., *Astrophys. J.* **678**, 594 (2008), 0801.1708.
 - [10] O. Adriani, G. C. Barbarino, G. A. Bazilevskaya, R. Bellotti, M. Boezio, E. A. Bogomolov, L. Bonechi, M. Bongi, V. Bonvicini, S. Bottai, et al., *ArXiv e-prints* (2008), 0810.4995.
 - [11] J. Chang, J. H. Adams, H. S. Ahn, G. L. Bashindzhagyan, M. Christl, O. Ganel, T. G. Guzik, J. Isbert, K. C. Kim, E. N. Kuznetsov, et al., *Nature (London)* **456**, 362 (2008).
 - [12] M. Cirelli, M. Kadastik, M. Raidal, and A. Strumia, *ArXiv e-prints* (2008), 0809.2409.
 - [13] N. Arkani-Hamed, D. P. Finkbeiner, T. R. Slatyer, and

- N. Weiner, ArXiv e-prints (2008), 0810.0713.
- [14] I. Cholis, L. Goodenough, D. Hooper, M. Simet, and N. Weiner, ArXiv e-prints (2008), 0809.1683.
- [15] F. Donato, D. Maurin, P. Brun, T. Delahaye, and P. Salati, ArXiv e-prints (2008), 0810.5292.
- [16] K. Ishiwata, S. Matsumoto, and T. Moroi, ArXiv e-prints (2008), 0811.0250.
- [17] A. Sommerfeld, *Annalen der Physik* **403**, 257 (1931).
- [18] L. Bergström, *Physics Letters B* **225**, 372 (1989).
- [19] J. Hisano, S. Matsumoto, and M. M. Nojiri, *Physical Review Letters* **92**, 031303 (2004), arXiv:hep-ph/0307216.
- [20] J. Hisano, S. Matsumoto, M. M. Nojiri, and O. Saito, *Phys. Rev. D* **71**, 063528 (2005), arXiv:hep-ph/0412403.
- [21] S. Profumo, *Phys. Rev. D* **72**, 103521 (2005), arXiv:astro-ph/0508628.
- [22] M. Lattanzi and J. Silk, ArXiv e-prints (2008), 0812.0360.
- [23] J. March-Russell, S. M. West, D. Cumberbatch, and D. Hooper, *JHEP* **7**, 58 (2008), 0801.3440.
- [24] J. March-Russell and S. M. West, ArXiv e-prints (2008), 0812.0559.
- [25] F. Chen, J. M. Cline, and A. R. Frey, ArXiv e-prints (2009), 0901.4327.
- [26] I. Büsching, O. C. de Jager, M. S. Potgieter, and C. Venter, *Astrophys. J. Lett.* **678**, L39 (2008), 0804.0220.
- [27] S. Profumo, ArXiv e-prints (2008), 0812.4457.
- [28] J. Dubinski and R. G. Carlberg, *Astrophys. J.* **378**, 496 (1991).
- [29] J. F. Navarro, C. S. Frenk, and S. D. M. White, *Astrophys. J.* **462**, 563 (1996), arXiv:astro-ph/9508025.
- [30] C. Boehm, D. Hooper, J. Silk, M. Casse, and J. Paul, *Physical Review Letters* **92**, 101301 (2004), arXiv:astro-ph/0309686.
- [31] A. Klypin, H. Zhao, and R. S. Somerville, *Astrophys. J.* **573**, 597 (2002), arXiv:astro-ph/0110390.
- [32] L. E. Strigari, S. M. Koushiappas, J. S. Bullock, M. Kaplinghat, J. D. Simon, M. Geha, and B. Willman, *Astrophys. J.* **678**, 614 (2008), 0709.1510.
- [33] J. F. Navarro, E. Hayashi, C. Power, A. R. Jenkins, C. S. Frenk, S. D. M. White, V. Springel, J. Stadel, and T. R. Quinn, *Mon. Not. R. Astron. Soc.* **349**, 1039 (2004), arXiv:astro-ph/0311231.
- [34] J. Einasto, *Astrofizika* **5**, 137 (1969).
- [35] J. Binney and S. Tremaine, *Galactic dynamics* (Princeton, NJ, Princeton University Press, 1987, 747 p., 1987).
- [36] J. Magorrian and J. Binney, *Mon. Not. R. Astron. Soc.* **271**, 949 (1994).
- [37] M. Geha, B. Willman, J. D. Simon, L. E. Strigari, E. N. Kirby, D. R. Law, and J. Strader, ArXiv e-prints (2008), 0809.2781.
- [38] V. Belokurov, D. B. Zucker, N. W. Evans, J. T. Kleyna, S. Koposov, S. T. Hodgkin, M. J. Irwin, G. Gilmore, M. I. Wilkinson, M. Fellhauer, et al., *Astrophys. J.* **654**, 897 (2007), arXiv:astro-ph/0608448.
- [39] G. D. Martinez, J. S. Bullock, M. Kaplinghat, S. E. Kaplinghat, and R. Trotta, ArXiv e-prints (2009), 0902.4715.
- [40] M. Kuhlen, J. Diemand, and P. Madau, *Astrophys. J.* **686**, 262 (2008), arXiv:0805.4416.
- [41] V. Springel, S. D. M. White, C. S. Frenk, J. F. Navarro, A. Jenkins, M. Vogelsberger, J. Wang, A. Ludlow, and A. Helmi, *Nature (London)* **456**, 73 (2008), arXiv:0809.0894.
- [42] L. M. Widrow and J. Dubinski, *Astrophys. J.* **631**, 838 (2005), arXiv:astro-ph/0506177.
- [43] S. Profumo, K. Sigurdson, and M. Kamionkowski, *Physical Review Letters* **97**, 031301 (2006), arXiv:astro-ph/0603373.
- [44] M. Kamionkowski and S. Profumo, *Physical Review Letters* **101**, 261301 (2008).